Chapter 3

Lanthanum cholate: A novel adsorbent for fluoride removal

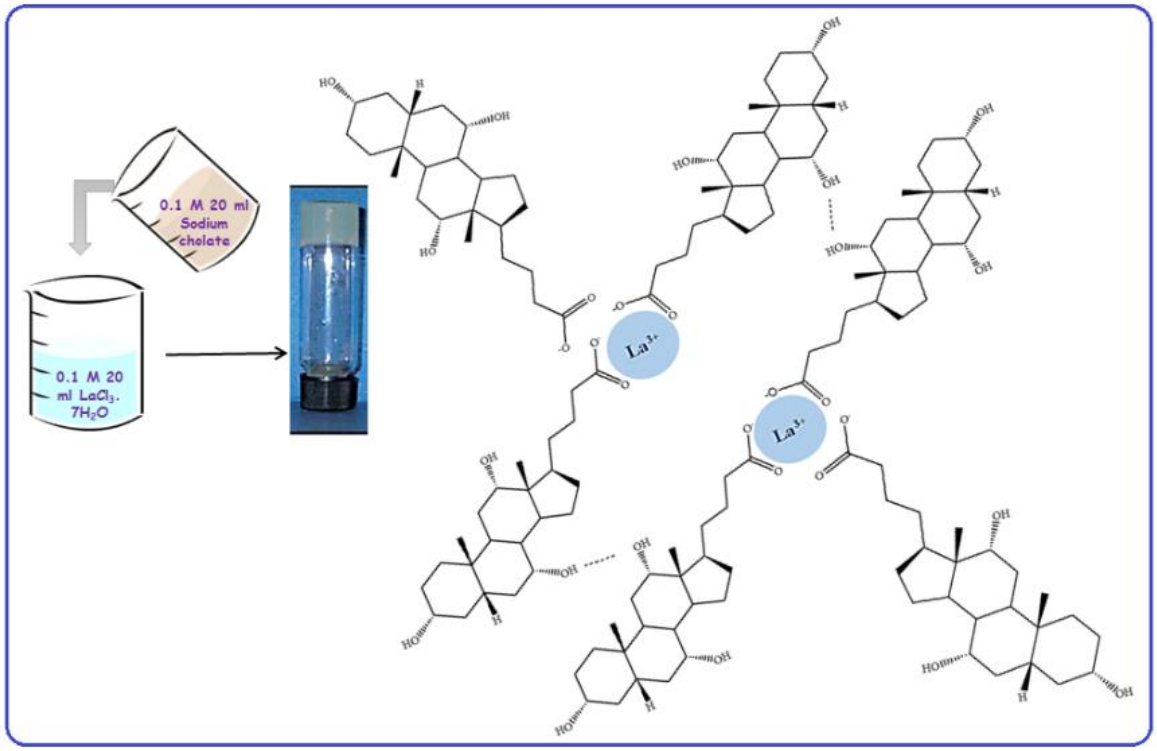

3.1 Introduction

Rare-earth metal-based adsorbents have recently been the subject of intensive research in the water treatment industry due to their abundant surface functional groups, high adsorption/catalytic performance and status as an advanced material class (Yu et al., 2018)(Li et al., 2018). Lanthanum (La), a rare-earth metal, is the second most common element after cerium (Herrmann et al., 2016). It has a particularly strong affinity for several contaminants, including fluoride, phosphate and arsenic.

It only manifests as a La^{3+} ion due to the exceptionally stable inert gas configuration and the f^0 configuration. La finds it difficult to form complexes with a coordination ligand, with the exception of very strong ligands, because there is no electron in the f orbital (e.g., oxygen-containing ligands). The contact between the La^{3+} ion and ligand are typically electrostatic attraction, which is akin to an ionic bond, because the size of the La^{3+} ion in the inert gas state is rather big.

La is one of the most effective elements for adsorbing contaminants from wastewater because of its high adsorption density (the molar ratio of an adsorbate to La). Typically, La species have a large pH range of operation and a high clearance rate (Dong & Wang, 2016).

Huo et al. prepared a lanthanum alginate bead adsorbent with a capacity of 197.2 mg/g for removal of fluoride (Huo et al., 2011). The beads were of amorphous nature and had homogenous adsorption sites. Vences et al. anchored lanthanum oxyhydroxides onto a commercial granular activated carbon (GAC) to remove fluoride from water with a maximum adsorption capacity of 9.98 mg/g. However, concentrations of co-existing anions greater than 30 mg/L had a negative effect on the fluoride adsorption capacity (Vences-Alvarez et al., 2015).

Wang et al. used lanthanum-modified bone waste to remove fluoride from water (Wang et al., 2017). Xu et al. created a hydrotalcite like material Mg/Fe/La in order to remove fluoride from water (Xu et al., 2017). Habibi et al. added La to *Tamarix hispida* charcoal to increase its potential to bind fluoride (Habibi et al., 2019). Jeyaseelan et al. employed a lanthanum and cerium based MOF containing benzene tricarboxylic acid to remove fluoride (Jeyaseelan & Viswanathan, 2021). E. E. Morales examined how surface characteristics affected the introduction of lanthanum and cerium functions in chars and activated carbons for fluoride and arsenic ion adsorption from aqueous solution (Merodio-Morales et al., 2020). Esmeralda

Vences-Alvarez anchored lanthanum oxyhydroxides on a commercial granular activated carbon to remove fluoride from water (Vences-Alvarez et al., 2015).

Shahin Ahmadi et al. attempted sono-chemical synthesis of $LaFeO_3$ nanoparticles for fluoride removal (Ahmadi et al., 2021). A. K. D. Veromee Kalpana Wimalasiri et al. fabricated hydroxyapatite with La and Ce ions to develop Lanthanide incorporated nano hydroxyapatite (Wimalasiri et al., 2021). They prepared composites having different ratio of La and Ce ions to enhance the fluoride removal from contaminated water. Yanyang Zhang et al. studied the behaviour and mechanism of lanthanum based nanomaterials for fluoride removal (Yanyang Zhang et al., 2019). They studied $La(OH)_3$, $La_2O_3 \cdot nH_2O$ and $LaCO_3OH$ species for uptake of fluoride.

Lizhi He et al. used municipal sludge to develop lanthanum-doped activated carbon for fluoride uptake from waste water. La/Mg/Si-activated carbon was developed by Minhee Kim et al. for simultaneous removal of fluoride and aluminium (Kim et al., 2020). They observed that it has rough and porous flocculent structure which was homogeneously modified by impregnation with La Mg, and Si. Lingchao Kong et al. developed cost effective periclase-based process for the synthesis of novel Mg-La bimetal oxide nanocomposite (Kong et al., 2020). Due to the inner sphere complex of nanocomposite, the adsorption of fluoride and phosphorus was achieved.

La-modified zeolite (LMZ) from coal fly ash was prepared by RenjieYang et al. for fluoride removal from waste water (Yang et al., 2022). The adsorbent was granulated with alginate for column studies. Vijoyeta Chakraborty et al. coated lanthanum oxide on biochar surface and investigated its efficiency for removal of fluoride (Chakraborty & Das, 2022).

Bile salts play an important biological role in the solubilization of cholesterol, lipids and fat-soluble vitamins. Sodium cholate (NaC) is one of the bile salts (figure 3.1). It is an amphiphilic molecule that forms aggregates in aqueous solution. Thus, NaC plays a role in the transportation and uptake of vital biological components. Bile salt-based hydrogels have been around for a while (Maitra et al., 2001). Sodium cholate being more soluble in water than the mono- and dihydroxy bile salts, the sodium salt of cholic acid (NaCh, 3-, 7-, and 12-trihydroxy) does not form a gel (Weiss & Terech, 2006). The rigid helical superstructures of the hydrogels are advantageous for the controlled formation of new nanomaterials, which could be used in biosensors, chiral catalysts, non-linear optics and material science, among other things (Sone et al., 2002). Yan Qiao et al. (Qiao et al., 2010) created temperature-

controlled, one-dimensional hierarchical designs via supramolecular self-assembly in the lanthanum-cholate system. These structures included nanotubes, coiled-coil, rope-like structures, nanohelices and nanoribbons. The "heating-enhanced stiffness" and "heating-promoted gelation" behaviours are shown in these supramolecular hydrogels.

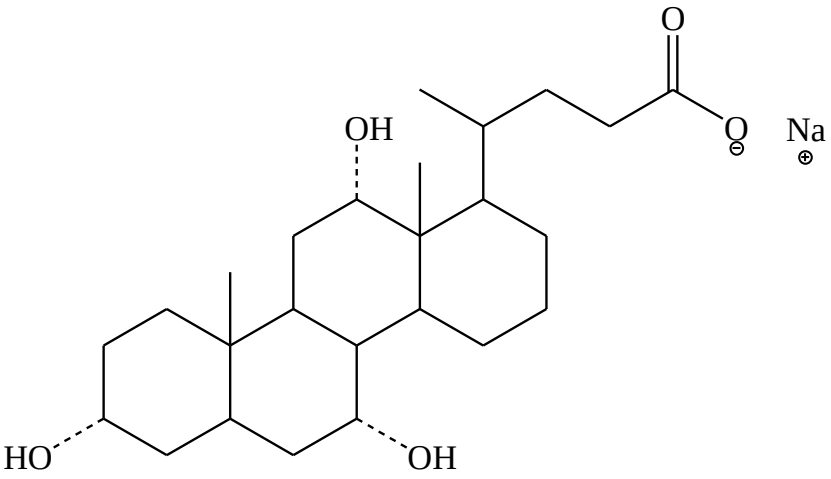

Figure 3.1 Chemical structure of Sodium cholate (Sodium (3-α, 5-β,7-α,12-α)-3,7,12-trihydroxycholan-24-oate)

Arkajyoti Chakrabarty et al. did detailed exploration of various metal cholate hydrogels with respect to their structure and properties (Chakrabarty et al., 2012). The supramolecular self-assemblies in the lanthanum-cholate system are thought to be explained by a variety of weak molecular interactions, including the hydrophobic effect, metal-ligand cooperation and hydrogen bonding. The structural basis of temperature-dependent lanthanum cholate self-assembly is thought to be the temperature-mediated hydrogen bonding between water and cholate. Furthermore, lanthanum, a rare earth metal categorised as a hard acid, has a strong affinity for fluoride ions (Yahui Zhang et al., 2016). Colloidal lanthanum, for instance, has been used to remove fluoride from water, but its usage in water treatment systems is highly problematic since it would be challenging to recover the adsorbent after fluoride adsorption at the end of the treatment (Na & Park, 2010; Rao & Karthikeyan, 2012; Thakre et al., 2010; Tomar & Kumar, 2013).

In the current study, sodium cholate, a bile salt, was initially utilised to create a gel with lanthanum (LaC), and its potential as an adsorbent for the removal of fluoride was examined.

3.2 Materials and methods

3.2.1 Materials

All chemicals utilised in this investigation, including NaF, Cholic acid sodium salt, $LaCl_3.nH_2O$, NaOH, HCl, NaCl, $NaHCO_3$, Na_2CO_3, $NaNO_3$ and Na_2SO_4 of analytical grade were obtained from Spectrochem in India and without additional processing. In order to create a fluoride stock solution (1000 mg/L), deionized water was combined with NaF (0.2210 g) (100 mL). The test solutions were created by properly diluting the typical stock solution.

3.2.2 Synthesis of Lanthanum cholate self-assembly

Sodium cholate and lanthanum chloride heptahydrate were simply mixed in an equal proportion to create the self-assembly of the hydrogel lanthanum cholate (LaC). To study the hydrogelation, the inverted test tube method was used. The resulting opaque hydrogel was further dried at 105°C and pulverised for use in fluoride adsorption tests. The synthesized hydrogel was characterized by methods such as Zeta potential, XRD, SEM-EDAX, FT-IR, TGA, DSC, XPS as described in chapter 2.

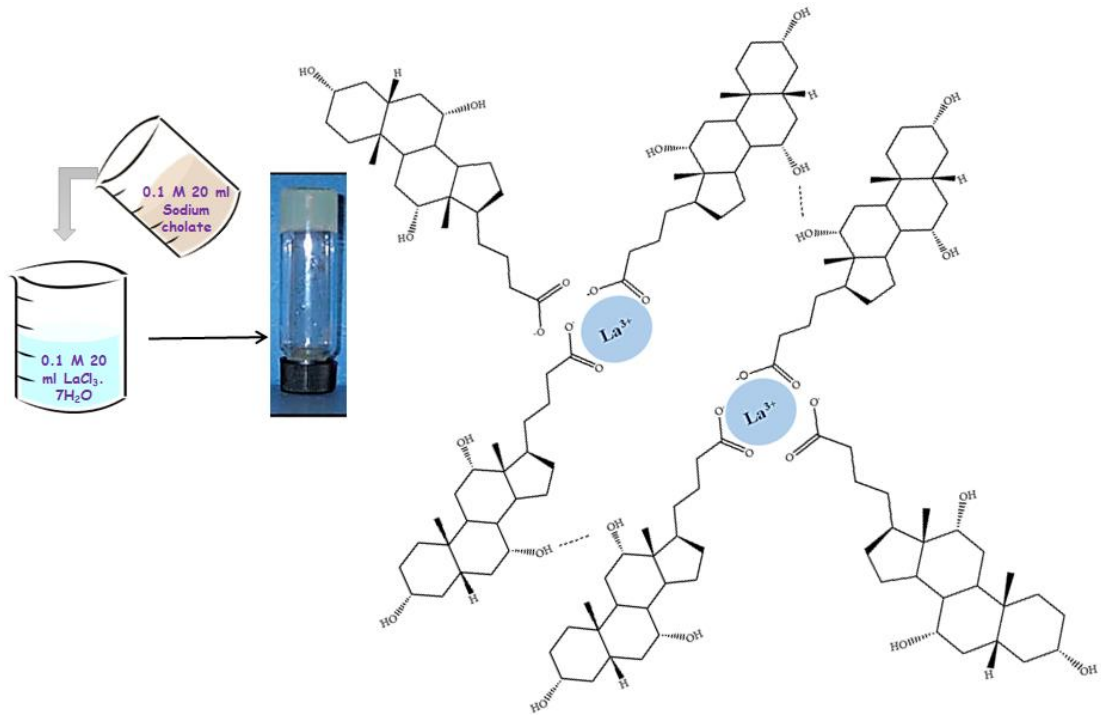

Figure 3.2 Synthesis of lanthanum-cholate assembly

3.2.3 Adsorption experiments and methods

The adsorptive potential of Lanthanum cholate for fluoride removal was investigated by batch adsorption technique. The pH of the solutions was adjusted to the desired value either

by 0.1 N NaOH or HCl. For the batch tests, 100 mL polypropylene flasks containing 100 mg/L of fluoride at neutral pH under ambient temperature (25-32^{o}C) conditions was agitated in an orbital shaker at 150 rpm for three hours to achieve equilibrium. Following fluoride uptake, the adsorbent was filtered out and dried for further investigation. Fluoride ion selective electrode was used to measure the amount of fluoride that was still unabsorbed in the filtrate (Thermo scientific ORION STAR A214). By analysing a series of solutions with a known concentration of fluoride, the instrument's calibration allowed for the determination of the unknown fluoride concentration. To keep the pH between 5-7 throughout the analysis, TISAB buffer was added at a ratio of around 5 mL/50 mL of the fluoride-containing solution.

The formula qe=Ci-Ce/m*100 was used to calculate the quantity of fluoride uptake. where qe is the amount of fluoride adsorbed per gram, Ci is the initial fluoride concentration per litre, Ce is the equilibrium fluoride concentration per litre, V is the volume of solution per litre, and m is the mass of the material (mg). With the exception of pH variation studies, all tests were carried out at pH 7. To comprehend the adsorption process, multiple isotherm and kinetic models were studied.

3.3 Results and discussion:

3.3.1 Characterisation of LaC

Figure 3.3 depicts the XRD spectra of LaC. The spectra of LaC showed discrete diffraction peaks at 16.1, 26.2, 30.4, 39.8, 46.8, and 56.2°, which were attributed to the lanthanum lattice planes (001), (100), (101), (102), (110), and (112). Similar peaks were observed by researchers in lanthanum modified carbon and lanthanum modified bone waste (Huong et al., 2019; Wang et al., 2017).

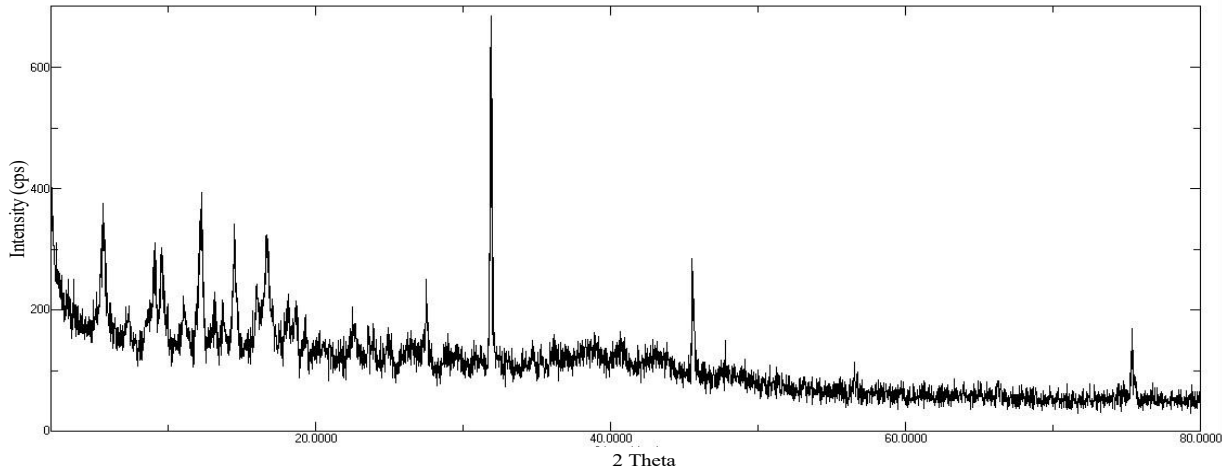

Figure 3.3 XRD spectra of LaC

After adsorption, the EDAX spectra (figure 3.4) affirmed the existence of La in LaC as well as Lanthanum and Fluoride.

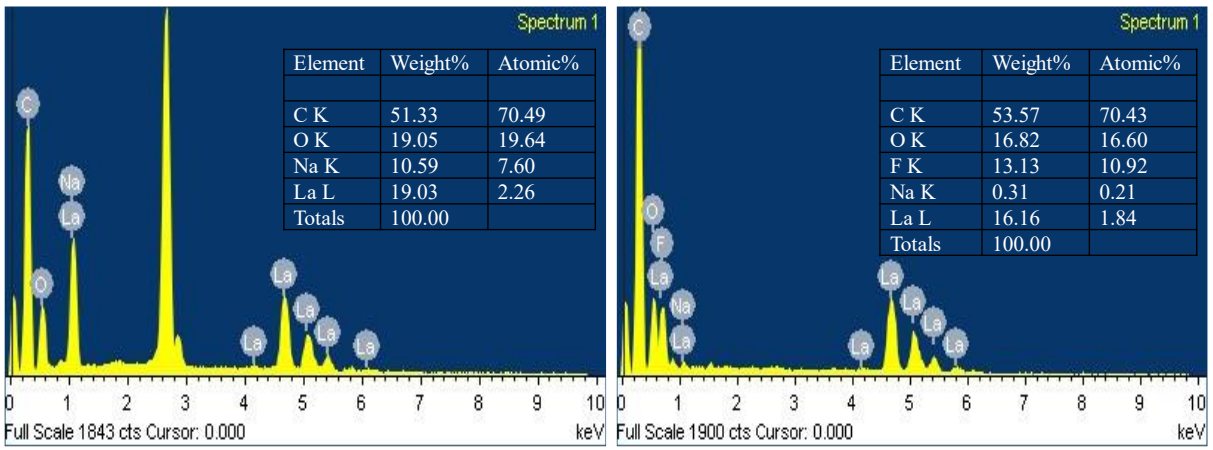

Figure 3.4 EDAX of LaC and LaCF

The Scanning electron micrograph (figure 3.5) showed that LaC was fibrous. The twisted ribbons were around 15 micrometres long. After fluoride adsorption, the fibrillar network of cholate was seen to disintegrate.

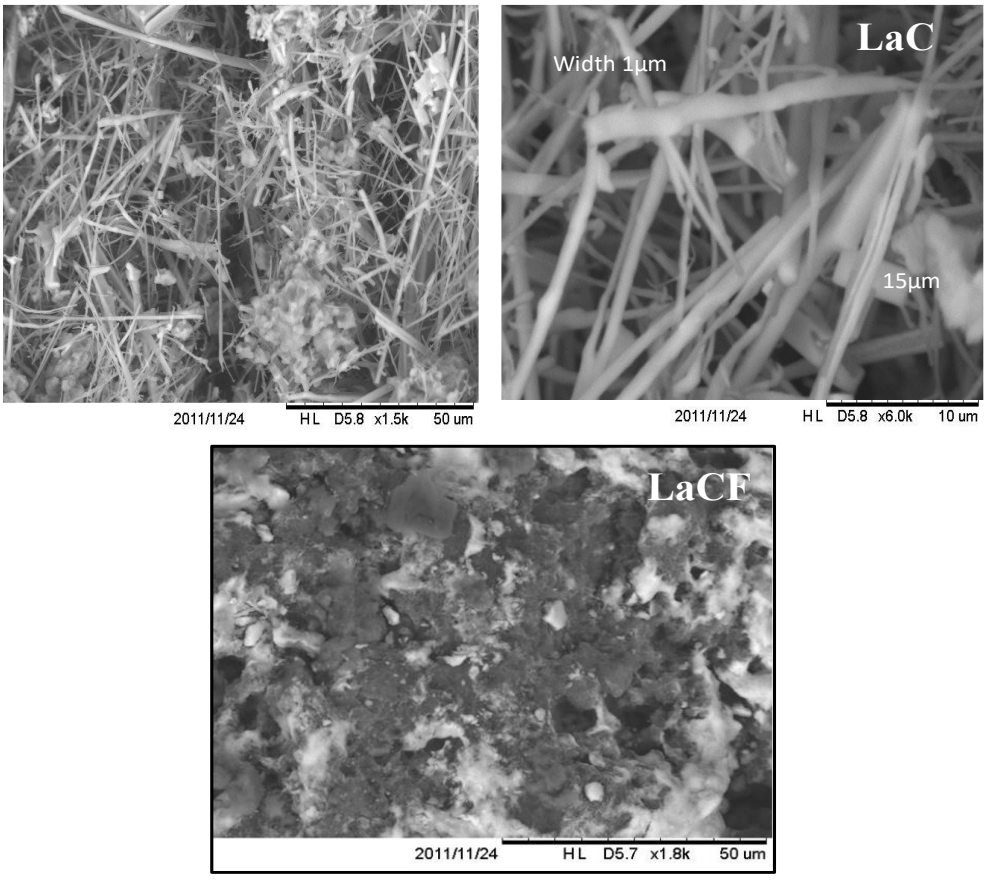

Figure 3.5 SEM images of LaC and LaCF

The thermogram of LaC (Figure 3.6) exhibited weight loss of 22.7% at ~234˚C attributed to disintegration of cholate network bound to lanthanum followed by a weight loss about 47.7% in the temperature range between 350 and 520^{o}C due to the decomposition of cholate molecules. The endothermic peak observed in the DSC thermogram may be attributed to the loss of supramolecular self-assembly network of Lanthanum cholate gel.

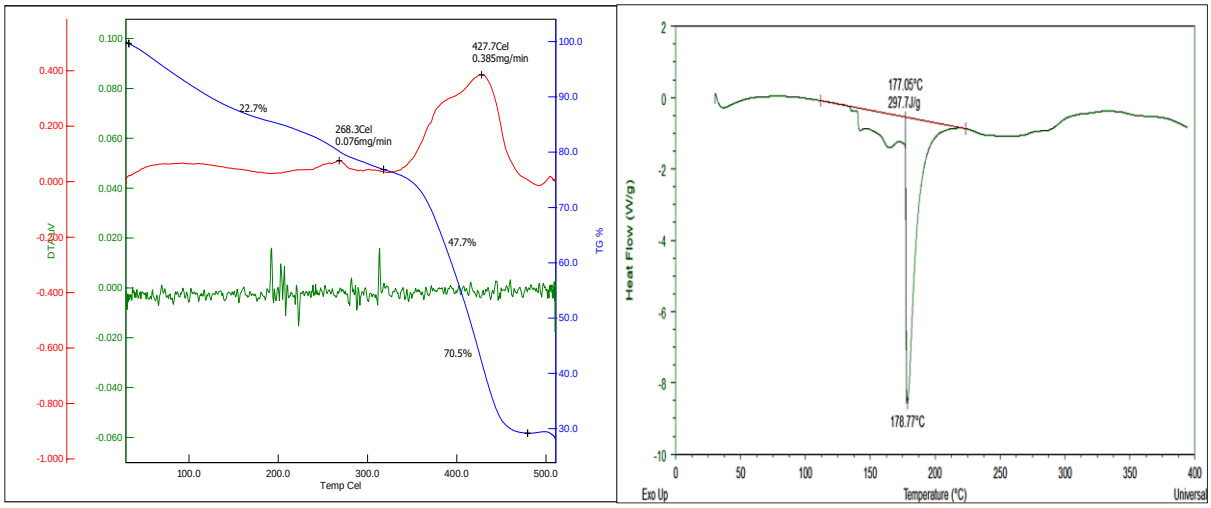

Figure 3.6 Thermogravimetric analysis and DSC of LaC

The FTIR spectra of sodium cholate, LaC, and LaCF are shown in Figure 3.7. The broad band in sodium cholate and Lanthanum cholate at 3380 cm^{-1} was ascribed to hydroxyl stretching mode (Qiao et al., 2010). The bands at 1578 and 1404 cm^{-1} in sodium cholate were ascribed to carboxyl asymmetric and symmetric stretching modes respectively, with a frequency separation Δν of 174 cm^{-1}. On the other hand, in lanthanum cholate, the absorption peaks were observed at 1536 and 1418 cm^{-1} respectively, wherein Δν is 118 cm^{-1} (figure 3.7b). The fact that lanthanum cholate's absorption frequencies were lower than sodium cholate's suggested that lanthanum interacted with carboxyl groups in a bidentate chelating manner. The assignment of bands at 1645, 856 cm^{-1} and 1039 cm^{-1} in LaC was to C=O, O-La stretching and C-O bending modes respectively.

Fluoride adsorption caused a blue shift from 3380 cm^{-1} to 3360 cm^{-1}, which may have been caused by a modification in the gel's structure. The absorption peaks at 1550 and 1409 cm^{-1} are observed for the anti-symmetric and symmetric stretching modes of carboxyl group respectively. The difference between these two frequencies is 139 cm^{-1} which is greater than that of pristine sodium cholate (118 cm^{-1}) indicating weakening of the La carboxylate binding. Further, the peak at 856 cm^{-1}, which was attributed to the La-O bond vibration, shifted to 861 cm^{-1} following adsorption indicating interaction between La-O and fluoride

during the adsorption process. It is possible to attribute the peak in LaCF at 562 cm^{-1} to La-F stretching vibration.

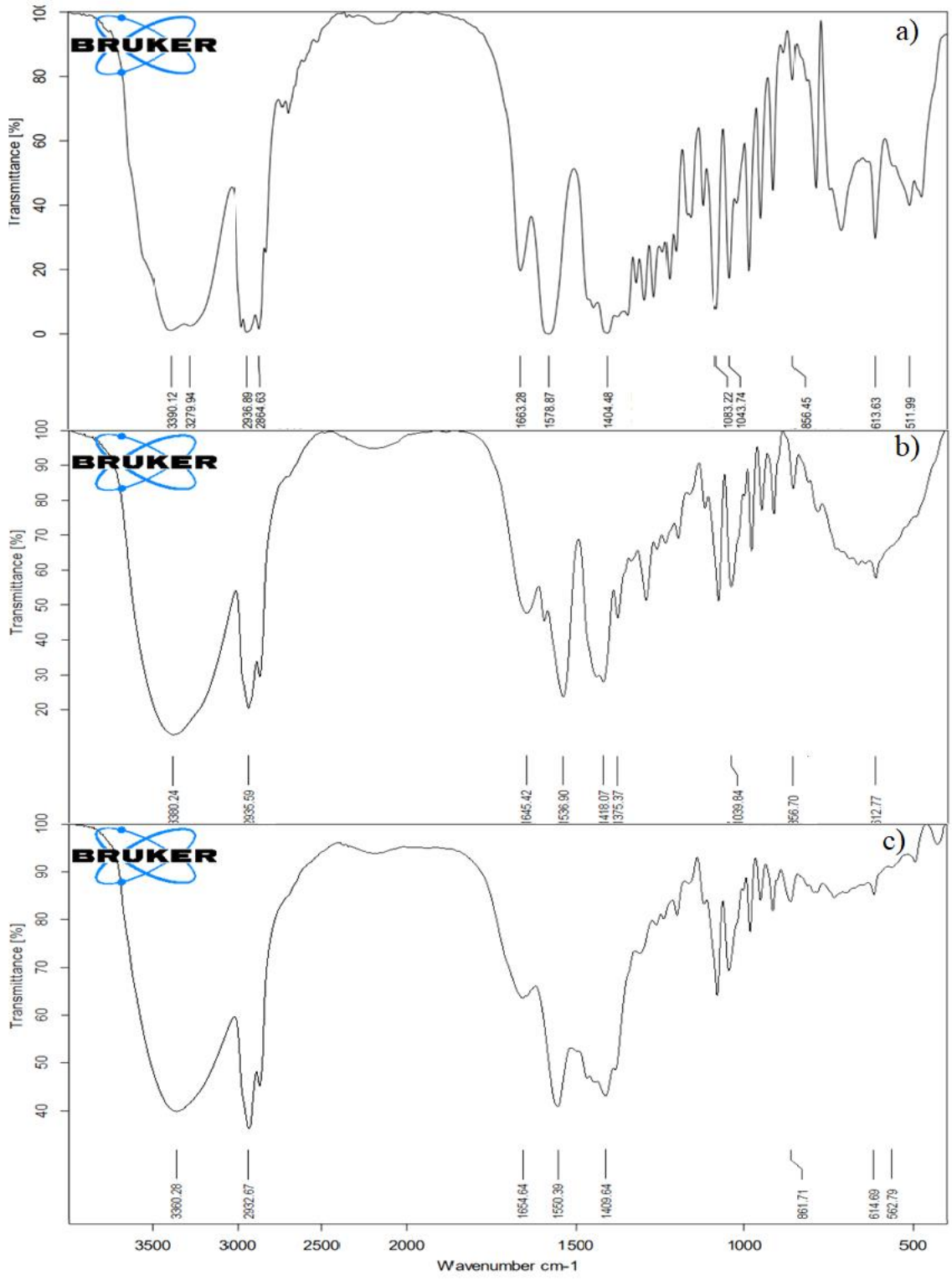

Figure 3.7 FTIR spectra of a) Sodium cholate, b) LaC and c) LaCF

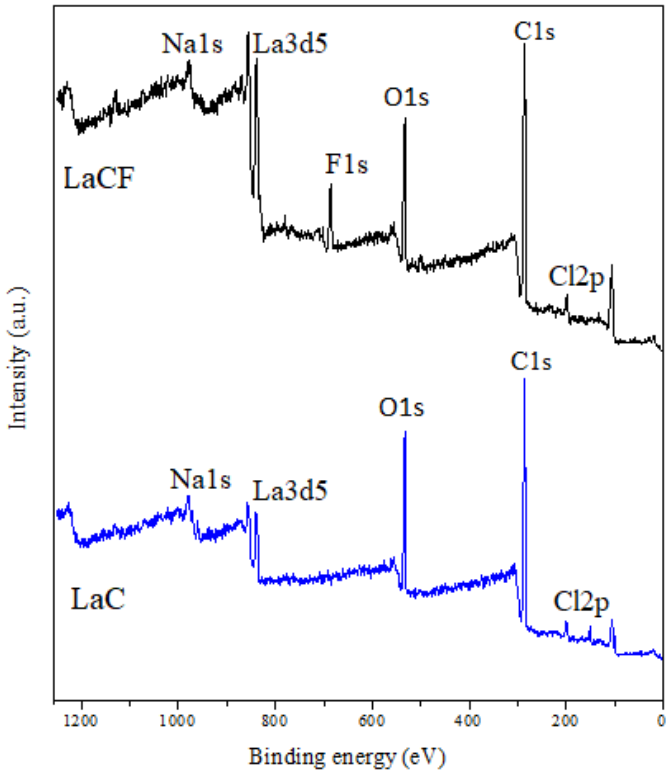

Figure 3.8 XPS spectra of LaC before and after adsorption of fluoride

The XPS spectra of LaC before and after fluoride adsorption are shown in Figure 3.8. The spectra showed peaks that were attributable to lanthanum (838 eV), sodium (1073 eV), oxygen (533 eV) and carbon (286 eV) (Patel et al., 2009). Fluoride was successfully adsorbed onto LaC as evidenced by the appearance of a new peak at 686.38 eV after the adsorption process.

3.3.2 Effect of solution pH

The effect of solution pH on fluoride adsorption onto 0.1 g of LaC was investigated using 25 mL of aqueous solution containing 50ppm fluoride and agitating for 3 hours. Figure 3.9b demonstrated that the adsorption process was pH independent. The PZC of LaC was observed to be at pH ~2 (figure 3.9a). The removal efficiency would have been maximum upto pH 2 if the removal process was electrostatic in nature due to $F^{-}\cdots OH_2^{+}$ interaction and would have decreased above pH 2 due to repulsion between O^{-} and F^{-}. The adsorption being independent of pH clearly indicated that some other mechanisms such as ion exchange, hard acid hard base interaction between Lanthanum and fluoride resulting in complex formation were also operating in the fluoride adsorption process.

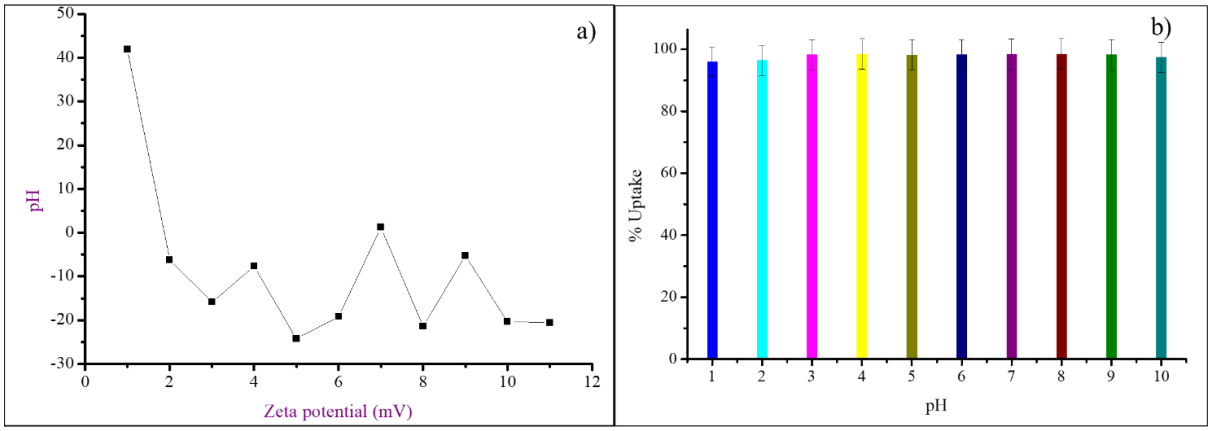

Figure 3.9 a) Zeta potential of LaC, b) Effect of pH on % uptake of fluoride (dose: 0.05 g, time: 3 h, conc.: 50 ppm)

3.3.3 Effect of adsorbent dose

The effect of dose of LaC on fluoride uptake at fixed initial concentration of fluoride is shown in figure 3.10. It was observed that as LaC dose increased the percentage uptake of fluoride increased.

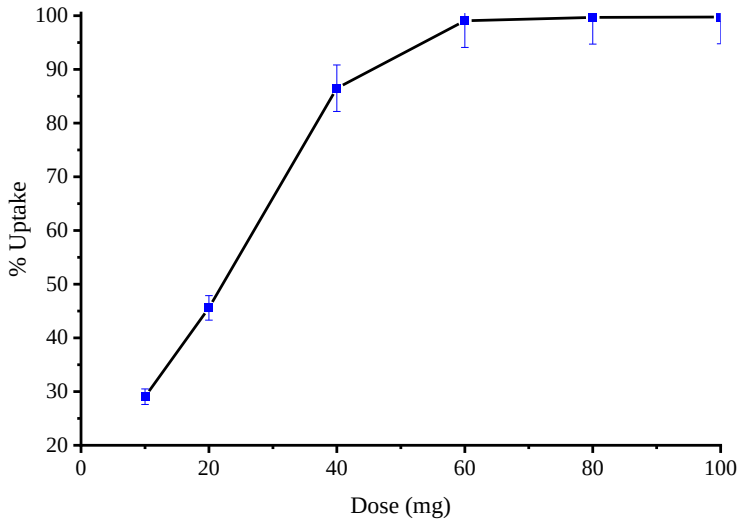

Figure 3.10 Effect of dose on % uptake of fluoride (time: 3 h, conc.: 100 mg/L),

3.3.4 Adsorption kinetic studies

The fluoride adsorption kinetics was studied by equilibrating 25 mL of solution containing 100 mg/L of fluoride, under neutral conditions for different time intervals with 50 mg of LaC (figure 3.11). Significant removal of fluoride occurred in the first 20 minutes (73%), followed by slow attainment of equilibrium in 3 h. The initial fast adsorption might be due to vacant adsorption sites in the presence of a high solute concentration gradient followed by a slow rate due to occupancy of the available adsorption sites (Patel et al., 2009).

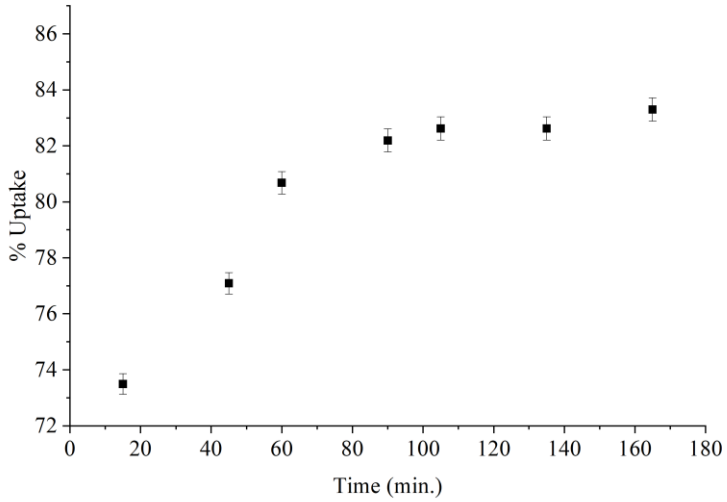

Figure 3.11 Effect of contact time on % uptake of fluoride (dose: 0.05 g, conc.: 50 mg/L)

The adsorption kinetic data (Table 3.1) exhibited a close correlation of experimental q_e values with calculated q_e values when fitted to pseudo-second order model indicating a diffusion-controlled process. The intraparticle diffusion model indicated that fluoride adsorption onto LaC involved two steps - rapid fluoride adsorption onto LaC in the first 20 min by boundary layer or macro-pore diffusion followed by a slow intraparticle or micro-pore diffusion attaining equilibrium.

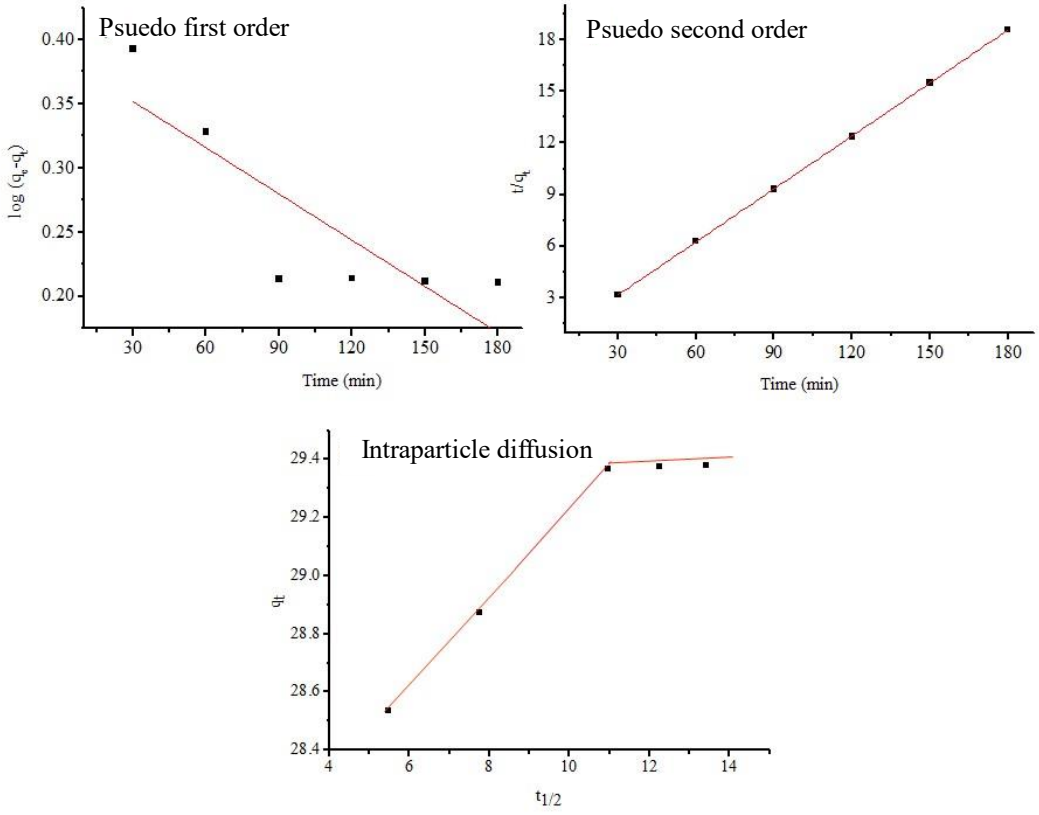

Figure 3.12 Kinetic models for fluoride adsorption onto LaC

Table 3.1 Kinetic parameters

q_e(exp): 29.38 mg/g	q_e	K	r^2
Pseudo First order	3.4158	0.0483	0.8443
Pseudo Second order	29.585	0.0371	1.0

3.3.5 Adsorption isotherm studies

Figure 3.13 depicts the effect of initial fluoride concentration (10 to 200 mg/L) on the adsorption process.

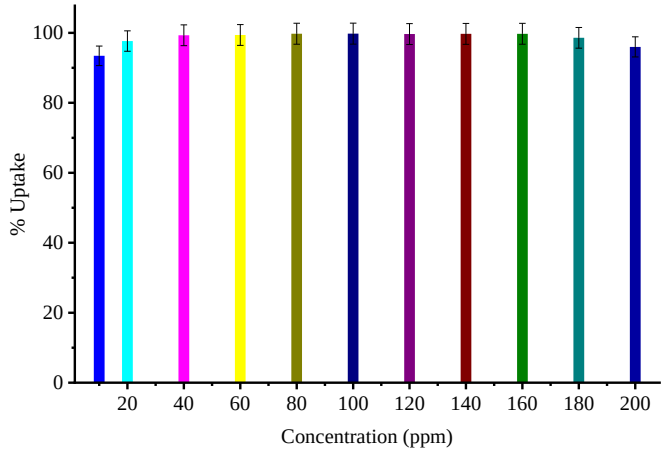

Figure 3.13 Effect of initial fluoride concentration on % uptake of fluoride (time: 3 h, dose: 0.1 g)

Langmuir and Freundlich isotherm models were used to further analyse the data. Table 3.2 and figure 3.14 show the results of the experimental data fitting and its parameters.

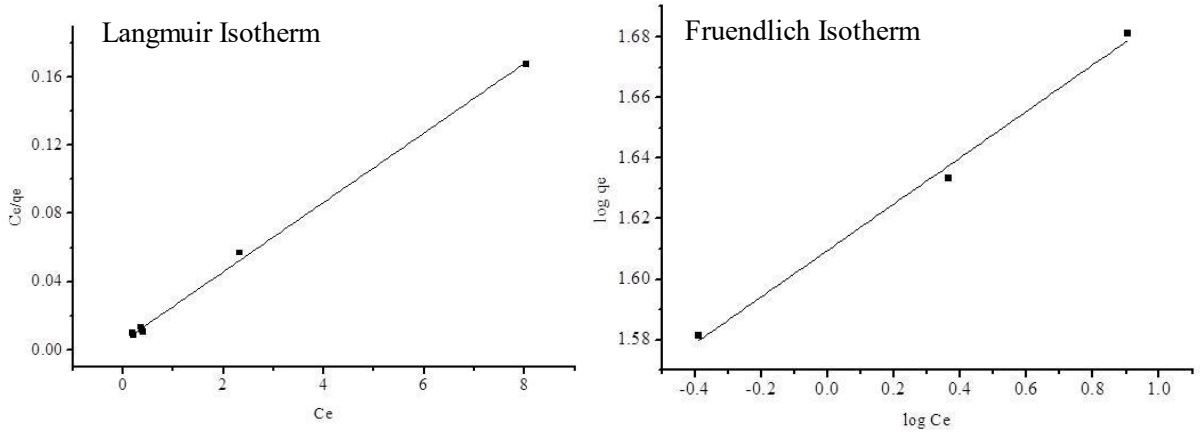

Figure 3.14 Isotherm models for fluoride adsorption onto LaC

The Langmuir model fitted the data better [r^2 = 0.99] than the Freundlich model [r^2 = 0.96], indicating that the adsorption occurred on a monolayer surface. The maximum adsorption capacity calculated from the Langmuir model (q_{max}) was 49.26 mg/g. When compared to adsorbents reported in the literature (Table 3.3), the adsorption capacity was comparable at neutral pH in a reasonable time interval of 3 h. Though adsorption was higher with some of the reported adsorbents, they either required more time to reach equilibrium or required acidic pH conditions, whereas LaC was effective as an adsorbent over a wide pH range (3-10). However, Mg/Fe/La CHLc hydrotalcite (Wu et al., 2017) and lanthanum-loaded magnetic cationic hydrogel composite (Dong & Wang, 2016) proved to be more effective adsorbents.

Table 3.2 Isotherm parameters

	Isotherm Parameters		
Langmuir	Q_m	K_L (L.mmol^{-1})	r^2
	49.26	3.9	0.99
Freundlich	N	k_F(L.g^{-1})	r^2
	13.42	40	0.96
Temkin	A_T (Lg^{-1})	b_T	r^2
	0.0574	-0.0902	0.89
Halsey	k_H (L.g^{-1})	n_H	r^2
	3.2*10^{21}	13.42	0.88

3.3.6 Effect of competing anions

In general, besides the anion of interest, the wastewater stream, ground water and various other sources of drinking water contain a number of other anions. As a result, studying fluoride uptake in the presence of other anions is highly desirable from an environmental standpoint. Fluoride uptake in the presence of other anions was investigated using 4 g/L adsorbent ratio in 50 mg/L fluoride solution containing chloride, sulphate, nitrate, carbonate and bicarbonate anions. Fluoride uptake was quantitative in the presence of 50 mg/L and 100 mg/L chloride, sulphate, nitrate, carbonate and bicarbonate anions, respectively (figure 3.15).

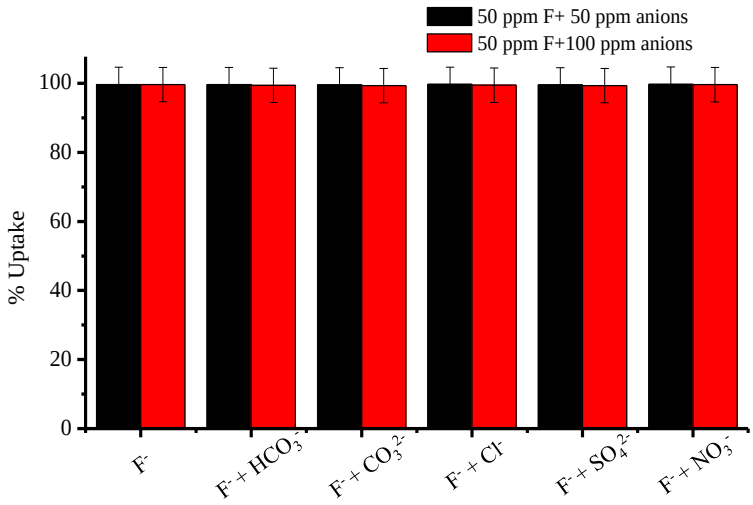

Figure 3.15 Effect of competing anion concentration on % uptake of fluoride

Table 3.3 Comparison of the fluoride maximum adsorption capacity by LaC with other reported adsorbents

Adsorbents	pH	q_e (mg/g)	Equilibrium time	References
Mg-Al-La hydrous oxide	7	41.746	40 min	(Hussain et al., 2015)
La-Alginate beads	4	197.2	24 h	(Huo et al., 2011)
Hybrid La-activated carbon	7	6.2	1 h	(Vences-Alvarez et al., 2015)
La modified seaweed	7	94.34	240 min	(Zhou et al., 2018)
Mg/Fe/La CHLc hydrotalcite like material	6.8	59.34	100 min	(Wu et al., 2017)
La modified bone waste	2.5-10	8.96	20 min	(Wang et al., 2017)
Lanthanum hydroxide	7.2	242.2	72 h	(Na & Park, 2010)
Lanthanum impregnated bauxite	7	18.8	120 min	(Vivek Vardhan & Srimurali, 2016)
Rose stem doped with Lanthanum	6.5	2.26	48 h	(García-Sánchez et al., 2018)
Zirconium–Lanthanum complexed polyvinyl alcohol films	7	11.57	45 min	(Metal., 2021)
lanthanum-loaded magnetic cationic hydrogel composite	7	136.78	10 min	(Dong & Wang, 2016)
Lanthanum aluminium perovskite	2	87.75	10 min	(Huang et al., 2021)
Lanthanum cholate	3-10	49.26	180 min	This study

3.4 Conclusions

In summary, LaC has been successfully synthesized for the first time and its surface nature and properties were investigated by XRD, XPS, TGA, EDAX, SEM and FTIR spectroscopic techniques. Efficient adsorption of fluoride by LaC occurred over a wide pH range with an adsorptive potential of 49.26 mg/g. LaC exhibited potential for de-fluoridation of ground water with no interference due to competing sulphate, carbonate, chloride, nitrate and bicarbonate ions.

In addition, the adsorption equilibrium was attained in about 3 h with maximum adsorption occurring within 20 minutes. The removal process may be by ion exchange and complex formation.

3.5 References

Ahmadi, S., Mesbah, M., Adaobi, C., Ezeliora, D., Osagie, C., Khan, N. A., Dotto, G. L., Salari, M., & Hadi, M. (2021). Journal of Environmental Chemical Engineering Sono electro-chemical synthesis of $LaFeO_3$ nanoparticles for the removal of fluoride : Optimization and modeling using RSM , ANN and GA tools. *Journal of Environmental Chemical Engineering*, *9*(4), 105320. https://doi.org/10.1016/j.jece.2021.105320

Chakrabarty, A., Maitra, U., & Das, A. D. (2012). Metal cholate hydrogels: Versatile supramolecular systems for nanoparticle embedded soft hybrid materials. *Journal of Materials Chemistry*, *22*(35), 18268–18274. https://doi.org/10.1039/c2jm34016j

Chakraborty, V., & Das, P. (2022). Investigation on efficiency of synthesized lanthanum oxide–coated biochar and graphene oxide–coated biochar on removal of fluoride: batch and fixed bed continuous reactor performance modelling. *Biomass Conversion and Biorefinery*, 1–14. https://doi.org/10.1007/s13399-022-02661-4

Dong, S., & Wang, Y. (2016). Characterization and adsorption properties of a lanthanum-loaded magnetic cationic hydrogel composite for fluoride removal. *Water Research*, *88*, 852–860. https://doi.org/https://doi.org/10.1016/j.watres.2015.11.013

García-Sánchez, J. J., Solache-Ríos, M., Ventura-Cruz, S., Martínez-Miranda, V., & Teutli-Sequeira, A. (2018). Fluoride removal behavior by aluminum-and lanthanum-doped bioadsorbents. *Desalination and Water Treatment*, *118*, 274–280. https://doi.org/10.5004/dwt.2018.22621

Habibi, N., Rouhi, P., & Ramavandi, B. (2019). Modification of Tamarix hispida Biochar by Lanthanum Chloride for Enhanced Fluoride Adsorption from Synthetic and Real Wastewater. *Environmental Progress and Sustainable Energy*, 298-305. https://doi.org/10.1002/ep.13026

Herrmann, H., Nolde, J., Berger, S., & Heise, S. (2016). Aquatic ecotoxicity of lanthanum – A review and an attempt to derive water and sediment quality criteria. *Ecotoxicology and Environmental Safety*, *124*, 213–238. https://doi.org/https://doi.org/10.1016/j.ecoenv.2015.09.033

Huang, L., Yang, Z., Lei, D., Liu, F., He, Y., Wang, H., & Luo, J. (2021). Experimental and modeling studies for adsorbing different species of fluoride using lanthanum-aluminum perovskite. *Chemosphere*, *263*, 128089. https://doi.org/https://doi.org/10.1016/j.chemosphere.2020.128089

Huo, Y., Ding, W., Huang, X., Xu, J., & Zhao, M. (2011). Fluoride removal by lanthanum alginate bead: Adsorbent characterization and adsorption mechanism. *Chinese Journal of Chemical Engineering*, *19*(3), 365–370. https://doi.org/10.1016/S1004-9541(09)60222-6

Huong, P. T., Jitae, K., Giang, B. L., Nguyen, T. D., & Thang, P. Q. (2019). Novel lanthanum-modified activated carbon derived from pine cone biomass as ecofriendly bio-sorbent for removal of phosphate and nitrate in wastewater. *Rendiconti Lincei*, *30*(3), 637–647. https://doi.org/10.1007/s12210-019-00827-3

Hussain, Z., Daosheng, L., Xi, L., & Jianxiong, K. (2015). Defluoridation by a Mg-Al-La triple-metal hydrous oxide: Synthesis, sorption, characterization and emphasis on the neutral pH of treated water. *RSC Advances*, *5*(55), 43906–43916. https://doi.org/10.1039/c5ra05539c

Jeyaseelan, A., & Viswanathan, N. (2021). Facile synthesis of tunable rare earth based metal organic frameworks for enhanced fluoride retention. *Journal of Molecular Liquids*, *326*, 115163. https://doi.org/10.1016/j.molliq.2020.115163

Kim, M., Choong, C. E., Hyun, S., Park, C. M., & Lee, G. (2020). Mechanism of simultaneous removal of aluminum and fluoride from aqueous solution by La/Mg/Si-activated carbon. *Chemosphere*, *253*, 126580. https://doi.org/10.1016/j.chemosphere.2020.126580

Kong, L., Tian, Y., Pang, Z., Huang, X., Li, M., Li, N., Zhang, J., Zuo, W., & Li, J. (2020). Needle-like Mg-La bimetal oxide nanocomposites derived from periclase and lanthanum for cost-effective phosphate and fluoride removal: Characterization, performance and mechanism. *Chemical Engineering Journal*, *382* 122963. https://doi.org/10.1016/j.cej.2019.122963

Li, S., Zhou, Y., Peng, Q., Wang, R., Feng, X., Liu, S., Ma, X., Ma, N., Zhang, J., Chang, Y., Zheng, Z., & Chen, X. (2018). Controllable Synthesis and Catalytic Performance of Nanocrystals of Rare-Earth-Polyoxometalates. *Inorganic Chemistry*, *57*(11), 6624–6631. https://doi.org/10.1021/acs.inorgchem.8b00763

M, S. K., Bhandari, R., Nehra, A., Manohar, C. S., & Belliraj, S. K. (2021). Zirconium–Cerium and Zirconium–Lanthanum complexed polyvinyl alcohol films for efficient fluoride removal from aqueous solution. *Journal of Dispersion Science and Technology*, *42*(10), 1550–1565. https://doi.org/10.1080/01932691.2020.1774386

Maitra, U., Mukhopadhyay, S., Sarkar, A., Rao, P., & Indi, S. S. (2001). Hydrophobic pockets in a nonpolymeric aqueous gel: Observation of such a gelation process by color change. *Angewandte Chemie - International Edition*, *40*(12), 2281–2283. https://doi.org/10.1002/1521-3773(20010618)40:12<2281::AID-ANIE2281>3.0.CO;2-L

Merodio-Morales, E. E., Reynel-Ávila, H. E., Mendoza-Castillo, D. I., Duran-Valle, C. J., & Bonilla-Petriciolet, A. (2020). Lanthanum- and cerium-based functionalization of chars and activated carbons for the adsorption of fluoride and arsenic ions. *International Journal of Environmental Science and Technology*, *17*(1), 115–128. https://doi.org/10.1007/s13762-019-02437-w

Na, C. K., & Park, H. J. (2010). Defluoridation from aqueous solution by lanthanum hydroxide. *Journal of Hazardous Materials*, *183*(1–3), 512–520. https://doi.org/10.1016/j.jhazmat.2010.07.054

Patel, G., Pal, U., & Menon, S. (2009). Removal of Fluoride from Aqueous Solution by CaO Nanoparticles. *Separation Science and Technology*, *44*(12), 2806–2826. https://doi.org/10.1080/01496390903014425

Qiao, Y., Lin, Y., Yang, Z., Chen, H., Zhang, S., Yan, Y., & Huang, J. (2010). Unique temperature-dependent supramolecular self-assembly: From hierarchical 1D nanostructures to super hydrogel. *Journal of Physical Chemistry B*, *114*(36), 11725–

11730. https://doi.org/10.1021/jp1047369

Rao, C. R. N., & Karthikeyan, J. (2012). Removal of fluoride from water by adsorption onto lanthanum oxide. *Water, Air, and Soil Pollution*, *223*(3), 1101–1114. https://doi.org/10.1007/s11270-011-0928-0

Sone, E. D., Zubarev, E. R., & Stupp, S. I. (2002). Semiconductor nanohelices templated by supramolecular ribbons. *Angewandte Chemie - International Edition*, *41*(10), 1705–1709. https://doi.org/10.1002/1521-3773

Thakre, D., Jagtap, S., Bansiwal, A., Labhsetwar, N., & Rayalu, S. (2010). Synthesis of La-incorporated chitosan beads for fluoride removal from water. *Journal of Fluorine Chemistry*, *131*(3), 373–377. https://doi.org/10.1016/j.jfluchem.2009.11.024

Tomar, V., & Kumar, D. (2013). A critical study on efficiency of different materials for fluoride removal from aqueous media. In *Chemistry Central Journal*, *7*(1), 1-15. https://doi.org/10.1186/1752-153X-7-51

Vences-Alvarez, E., Velazquez-Jimenez, L. H., Chazaro-Ruiz, L. F., Diaz-Flores, P. E., & Rangel-Mendez, J. R. (2015). Fluoride removal in water by a hybrid adsorbent lanthanum-carbon. *Journal of Colloid and Interface Science*, *455*, 194–202. https://doi.org/10.1016/j.jcis.2015.05.048

Vivek Vardhan, C. M., & Srimurali, M. (2016). Removal of fluoride from water using a novel sorbent lanthanum-impregnated bauxite. *SpringerPlus*, *5*(1), 1426. https://doi.org/10.1186/s40064-016-3112-6

Wang, L., Xie, Y., Yang, J., Zhu, X., Hu, Q., Li, X., & Liu, Z. (2017). Insight into mechanisms of fluoride removal from contaminated groundwater using lanthanum-modified bone waste. *RSC Advances*, *7*(85), 54291–54305. https://doi.org/10.1039/c7ra10713g

Weiss, R. G., & Terech, P. (2006). Molecular gels: Materials with self-assembled fibrillar networks. In *Molecular Gels: Materials with Self-Assembled Fibrillar Networks*. https://doi.org/10.1007/1-4020-3689-2

Wimalasiri, A. K. D. V. K., Fernando, M. S., Dziemidowicz, K., Williams, G. R., Koswattage, K. R., Dissanayake, D. P., De Silva, K. M. N., & De Silva, R. M. (2021). Structure-Activity Relationship of Lanthanide-Incorporated Nano-Hydroxyapatite for

the Adsorption of Fluoride and Lead. *ACS Omega*, *6*(21), 13527–13543. https://doi.org/10.1021/acsomega.0c05935

Wu, P., Wu, J., Xia, L., Liu, Y., Xu, L., & Song, S. (2017). Adsorption of fluoride at the interface of water with calcined magnesium-ferri-lanthanum hydrotalcite-like compound. *RSC Advances*, *7*(42), 26104–26112. https://doi.org/10.1039/c7ra04382a

Yang, R., Chen, J., Zhang, Z., & Wu, D. (2022). Performance and mechanism of lanthanum-modified zeolite as a highly efficient adsorbent for fluoride removal from water. *Chemosphere*, *307*, 136063. https://doi.org/https://doi.org/10.1016/j.chemosphere.2022.136063

Yu, Y., Wang, C., Guo, X., & Paul Chen, J. (2015). Modification of carbon derived from Sargassum sp. by lanthanum for enhanced adsorption of fluoride. *Journal of Colloid and Interface Science*, *441*, 113–120. https://doi.org/10.1016/j.jcis.2014.10.039

Yu, Y., Yu, L., Koh, K. Y., Wang, C., & Chen, J. P. (2018). Rare-earth metal based adsorbents for effective removal of arsenic from water: A critical review. *Critical Reviews in Environmental Science and Technology*, *48*(22–24), 1127–1164. https://doi.org/10.1080/10643389.2018.1514930

Zhang, Yahui, Lin, X., Zhou, Q., & Luo, X. (2016). Fluoride adsorption from aqueous solution by magnetic core-shell Fe3O4@alginate-La particles fabricated via electro-coextrusion. *Applied Surface Science*, *389*, 34–45. https://doi.org/10.1016/j.apsusc.2016.07.087

Zhang, Yanyang, Qian, Y., Li, W., Gao, X., & Pan, B. (2019). Fluoride uptake by three lanthanum based nanomaterials: Behavior and mechanism dependent upon lanthanum species. *Science of the Total Environment*, *683*, 609–616. https://doi.org/10.1016/j.scitotenv.2019.05.185

Zhou, Y., Zhang, H., Cai, L., Guo, J., Wang, Y., Ji, L., & Song, W. (2018). Preparation and characterization of macroalgae biochar nanomaterials with highly efficient adsorption and photodegradation ability. *Materials*, *11*(9). https://doi.org/10.3390/ma11091709